USING DEEP LEARNING FOR AUTOMATIC DEFECT DETECTION ON A SMALL WELD X-RAY IMAGE DATASET

Qingchun ZHENG[1,2], Xiaoyang LI[1,2], Peihao ZHU[1,2,*], Wenpeng MA[1,2]
Jingna LIU[1,2], Qipei LIU[1,2]

The quality of welding is directly related to the performance and life of welded products. This paper proposes an automatic defect detection method using deep learning on a small weld X-ray image dataset. Combined with Generative Adversarial Network (GAN) and Deep Convolutional Neural Network (DCNN), this method can successfully deal with the problem of data imbalance in small image dataset and achieves a good detection effect for low-contrast defect images. Extensive experiments have proved that this approach could accurately and quickly complete the location and detection task of internal defects of welds, and it achieves the Mean Average Precision (mAP) result as 91.64%.

Keywords: Deep learning, X-ray images, GAN, Data augmentation, Defect detection

1 Introduction

As a primary method of connecting workpieces, welding has been widely used in many fields such as equipment manufacturing, aerospace, petrochemical industry. In addition to welding efficiency and accuracy, welding production is also affected by welding quality. Due to the influence of different environmental conditions and welding processes, various defects will inevitably appear inside the weld during the welding process, such as cracks, pores, lack of penetration, slag inclusion [1]. In order to ensure the quality of welded products, it is imperative to conduct Non-Destructive Testing (NDT) before putting it into use.

NDT technology includes many methods. Radiographic Testing (RT) is one of the most commonly used NDT methods for welded defects, and it mainly consists of two methods: Manual visual detection and computer-aided detection [2]. At present, most industries use manual visual detection methods for testing. However, the manual visual detection method is greatly affected by personal subjective factors, and it is easy to cause misjudgment and omission. In recent

[1] Tianjin Key Laboratory for Advanced Mechatronic System Design and Intelligent Control, School of Mechanical Engineering, Tianjin University of Technology, Tianjin 300384, China
[2] National Demonstration Center for Experimental Mechanical and Electrical Engineering Education (Tianjin University of Technology)
[*] Corresponding author: Peihao Zhu, E-mail: 935746496@qq.com

years, computer vision and object detection technology have developed rapidly, and the computer-aided detection method has received more attention [3].

At present, the computer-aided detection method faces three main challenges: First of all, due to external noise interference, it is difficult to distinguish whether it is a noise or a defect with a smaller size in the weld image. Secondly, the types and characteristics of welding defects are diverse. Some welding defects with low contrast and uneven brightness are difficult to detect accurately. Third, it is costly to collect a lot of welded defect images in the industry, which leads to severe data imbalance problems [4].

This paper proposes an automatic detection method for weld defects based on a small image dataset to solve the above problems. The main contributions of this article are as follows: (1) In order to ensure the effectiveness of the object detection model, a Generative Adversarial Network (GAN) algorithm based on small image dataset is proposed to quickly generate high-quality welded defect images to expand the training dataset. (2) An object detection model of DCNN is proposed to realize the defect detection of the entire X-ray weld image. Experimental results show that this method's mean average precision (mAP) for the two defects reached 91.64%.

2 Related work

At present, the traditional three-stage defect detection method and the defect intelligent recognition method without feature extraction are the research hotspots.

Most of the traditional three-stage defect recognition methods belong to the category of machine learning, which requires manual design and extraction of features. The effect of classification mainly depends on the quality of feature extraction. Common image features include shape features, texture features, geometric features, and combined features [5].

In recent years, CNN has repeatedly achieved good results in object detection. The emergence of AlexNet [6] has attracted much attention, and VGGNet, GoolLeNet [7-8] network structures were subsequently proposed. The depth and width of the network continue to expand, and the error rate of classification is also declining. However, the above-mentioned CNNs are only suitable for image classification tasks and cannot meet the object detection of the entire image in the actual application scene.

With the continuous reduction of image classification error rate based on the ImageNet dataset, people have begun to consider improvements based on existing research to complete the object detection works. Du et al. [9] proposed an improved Faster R-CNN network structure, and it is the first time the FPN structure has been applied to defect detection and achieved an excellent detection

result. Lei Yang et al. [10] used the YOLO-V3 network to develop a welded joint detection system that updates the data in real-time.

However, the intelligent detection method of welded defects based on deep learning requires many images as training samples. With the increasing demand for the dataset in the industry, people have begun to use Generative adversarial network (GAN) [11] to generate weld images. Since GAN training is very unstable and prone to problems such as mode collapse, Martin Arjovsky [12] proposed an improved GAN called WGAN-GP in 2017.

3. A small weld x-ray image dataset

3.1 Image source

The public datasets and online collection are used to get X-ray images as training samples. Many X-ray images come from the public dataset GDXray. The GDXray dataset [13] was released by Domingo Mery et al. in 2015 and is the only publicly available X-ray weld image dataset. It contains 88 X-ray weld images, and there are problems in the dataset's number, quality, and data balance. At the same time, some samples were collected from online search engines.

Different types of weld defects have various features on X-ray images. Defects of “pores” type on the X-ray image are round defects or strip defects with deep black center and shallow black edge. The defects of “crack” type on the X-ray image are characterized by a black straight line with wide middle and sharp ends. In this paper, data augmentation and object detection are performed on the above two kinds of defects. Some real images of these two kinds of weld defects are shown in Fig. 1.

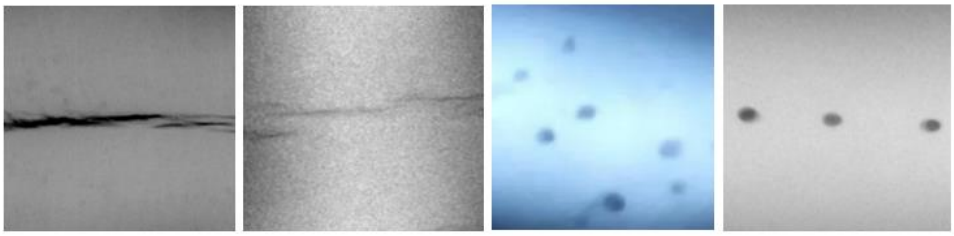

Fig. 1 Various kinds of defects

3.2 Image augmentation

Due to the quality problem of collected images, the two methods mentioned above still cannot obtain enough samples to meet the needs of the model. Therefore, this paper uses some image-processing-based algorithms for image augmentation, such as image flip, brightness enhancement and image noise.

(1) Image flip: Due to the different X-ray projection angles in industrial production, the angles of the X-ray images produced are also different. Therefore,

the image flip method is used to simulate the actual application of different angles of defect pose.

(2) Brightness enhancement: In the actual welding process, the light source changes will affect the imaging effect of the x-ray image. Here, the brightness enhancement is adopted to simulate the change of lighting conditions.

(3) Image noise: Due to the imperfections of the imaging system, digital images often have noise during the process of their formation. Here, the dataset is expanded by adding noise to the original image.

3.3 WGAN-GP network

The framework of WGAN-GP is shown in Fig. 2. The generator could learn feature information in real images to generate fake images to deceive Discriminator. It produces images that can replace real samples during the constant confrontation.

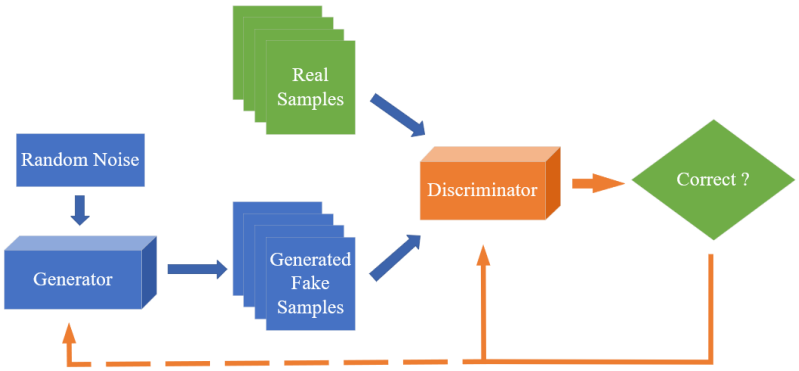

Fig. 2 Framework of WGAN-GP in this paper

WGAN-GP network uses Gradient Penalty (GP) instead of weight clipping. At the same time, in order to prevent the gradient value from being changed with the batch processing information, the Batch Normalization operation in the Discriminator is deleted. The gradient penalty is defined as Equation 1.

$$Gradient\ penalty = \lambda \mathrm{E}\hat{x}\left[\left(\left\|\nabla_{\hat{x}} D(\hat{x})\right\|_2 - 1\right)^2\right] \tag{1}$$

Where $\hat{x}$ is Linear interpolation between the real image and the generated fake image. $\nabla_{\hat{x}} D(\hat{x})$ is the gradient of Discriminator output relative to the interpolation. λ is the ratio of the gradient penalty to the Original critic loss.

WGAN-GP network solves three critical problems of WGAN network: insufficient network capacity usage, gradient vanishing and gradient exploding. Compared with other networks, the WGAN-GP network does not require any prior knowledge to generate defect samples.

3.4 Network structure optimization

To get better performance of the WGAN-GP network, this paper proposes to add the ResNet structure to the WGAN-GP network structure.

(1) Generator

The plain Generator structure is repeatedly stacked by Deconv_Block composed of Deconvolution layer, Batch Normalization layer and LeakyReLU activation function. The Deconv_Block structure is shown in Fig. 3 (a). The Deconvolution layer uses image interpolation to enlarge the original image. The batch normalization layer is used to stabilize training, speed up convergence and regularize the model.

In this paper, the shortcut connection is added based on the above-mentioned plain structure. At the same time, two Deconv_Block are used to enhance the upsampling ability of the model to obtain a clearer image. The optimized structure is called ResBlock_G, and the detailed structure is shown in Fig. 3 (a).

(2) Discriminator

The discriminator of the original WGAN-GP network deleted the Batch Normalization layer and only retained the convolutional layer and the LeakyReLU activation function. The structure of the original discriminator is shown as Conv_Block in Fig. 3 (b). The convolutional layer is used to subsampled the image to achieve the extraction of feature information.

The shortcut connection is also added to the original discriminator. It realizes the fusion of high-dimensional feature information and low-dimensional feature information and enhances the ability of the discriminator. The optimized structure is called ResBlock_D, and the detailed structure is shown in Fig. 3 (b).

Table 1

The final amount of generated data

Index	Image transformation	Number
1	Original image	270
2	Image flip	540
3	Brightness enhancement	270
4	Image noise	270
5	GAN network	203
6	Total images	1553

The improved WGAN-GP network can generate welded defects with different sizes, shapes and numbers. Combined with the improved WGAN-GP

network and image-processing-based algorithms, the final amount of generated data is shown in Table 1.

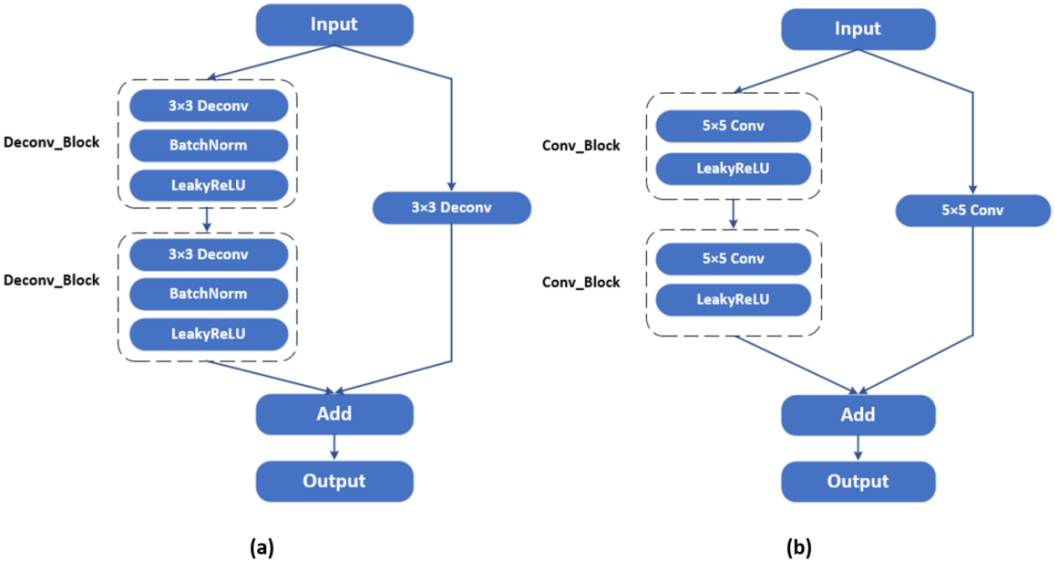

Fig. 3 Network structure. (a) Resblock_G; (b) Resblock_D

4 Weld defect detection

YOLO-V4 [14] model is currently the most widely used algorithm in the field of object detection. It is optimized from the YOLO-V3 model [15] and achieves a good balance between accuracy and speed. In order to obtain better object detection precision, the idea of feature pyramid networks (FPN) [16] is used to achieve the fusion of low-dim feature information and high-dim feature information. Fig. 4 shows the structure of YOLO-V4 model.

In terms of the loss function, the YOLO-V4 model uses CIOU directly as a regression to optimize loss function, taking into account the parameters between the object and the anchor, such as distance, overlap rate and penalty items. The CIOU is defined as shown in Equation 3.

$$CIOU = IOU - \frac{\rho^2(b, b^{gt})}{c^2} - \alpha\upsilon \tag{3}$$

Where $\rho^2(b, b^{gt})$ denotes the Euclidean distance between the center point of the predict bounding box and the ground-truth bounding box. C denotes the diagonal distance of the smallest closure area that can contain both the predict bunding box and the ground-truth bounding box. The parameters α and υ are shown in Equation 4 and Equation 5 respectively.

$$\alpha = \frac{\upsilon}{1 - IOU + \upsilon} \tag{4}$$

$$\upsilon = \frac{4}{\pi}(\arctan\frac{w^{gt}}{h^{gt}} - \arctan\frac{w}{h})^2 \tag{5}$$

Finally, the loss function of YOLO-V4 model is shown as Equation 6.

$$LOSS_{CIOU} = 1 - IOU + \frac{\rho^2(b, b^{gt})}{c^2} + \alpha\upsilon \tag{6}$$

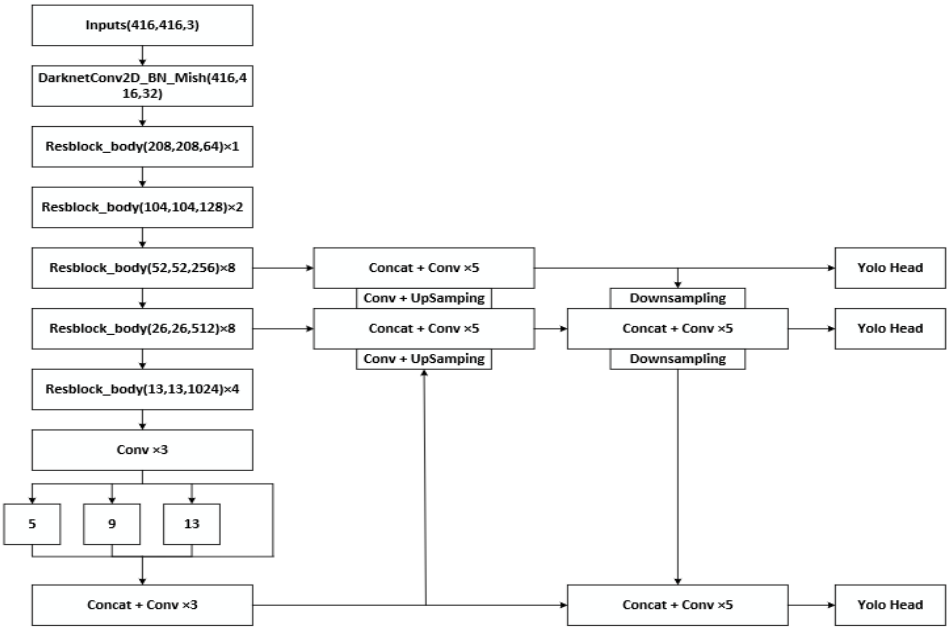

Fig. 4 The structure of YOLO-V4 model

5 Experiment and discussion

5.1 Evaluation indicators

In order to shorten the training time, the experiments are done on NVIDIA Quadro RTX 5000 to accelerate these two networks training. At the same time, some evaluating indexes are needed to prove the validity of the object detection model.

(1) Precision-Recall (P-R) Curve: The parameters precision (P) and recall (R) are defined as Equation 7 and Equation 8. In two-dimensional coordinates, the combination of P and R can generate a P-R curve.

$$\Pr ecision = \frac{TP}{TP + FP} \tag{7}$$

$$Racall = \frac{TP}{TP + FN} \tag{8}$$

Where TP denotes the number of positive samples that are correctly classified. FP represents the number of negative samples that are misclassified. FN denotes the number of positive samples incorrectly classified.

(2) F1 Score: F1 Score is the harmonic mean of precision and recall. Its value range is 0-1. 1 represents the best output result of the model, and 0 represents the worst output result of the model.

(3) Mean Average Precision (mAP): The Average Precision (AP) is the area enclosed by the P-R curve, the X-axis and the Y-axis. In this paper, there are two objects to be detected, and mAP is the mean value of the AP of pores and cracks.

5.2 Dataset augmentation

Before the WGAN-GP network training, some parameters need to be set in advance to ensure that the model achieves the expected results. The initialization parameters are shown in Table 2. Part of the generated results of the optimized WGAN-GP model and the original WGAN-GP model are shown in Fig. 5.

Table 2

The initialization parameters of WGAN-GP

Index	Parameters	Value
1	Image size	256*256
2	Batch size	8
3	Learning rate	2e-4
4	λ	10

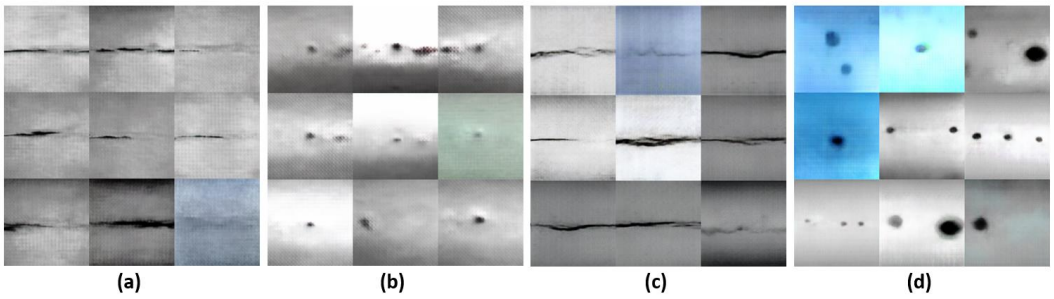

Fig. 5 Image augmentation based on WGAN-GP network

Fig. 5 (a-b) shows images of cracks and pores generated by the original WGAN-GP model. Fig. 5 (c-d) shows images of cracks and pores generated by the optimized WGAN-GP model. As shown in Fig. 5, the texture features of the defect images generated by the original WGAN-GP model are blurred, and the checkerboard pattern has appeared. However, the weld defect images generated

by the optimized WGAN-GP network have clearer texture feature information. It is evident that this method solves the problem of lacking samples of x-ray images, and the dataset of defects could be expanded to train the DCNN models.

5.3 Network training

Similar to the WGAN-GP network, we also set some initialization parameters for the YOLO-V4 model to obtain the desired results, as shown in Table 3.

Table 3

The initialization parameters of YOLO-V4 model

Index	Parameters	Value
1	Image size	416*416
2	Batch size	2
3	Learning rate	1e-4
4	Freeze epoch	50
5	Epoch	100

In the process of network training, this paper uses the freeze technique to speed up the convergence of the model while also preventing the weight from being destroyed. After many experiments, the training time of the model stabilizes at about 2 hours. Fig. 6 shows the Precision-Recall curve of the YOLO-V4 network.

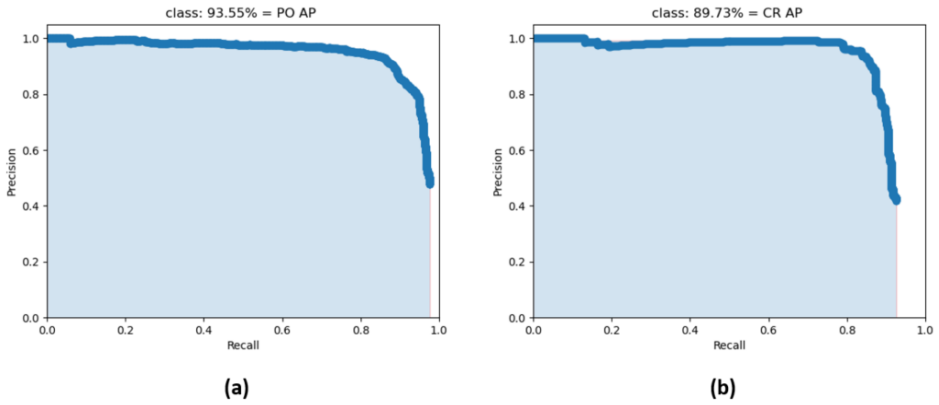

Fig 6 (a) The P-R curve of pores; (b) The P-R curve of cracks.

It can be seen from Fig. 8 that the average Precision of cracks and pores are 89.73% and 93.55%, respectively. The mean Average Precision (mAP) is 91.64%.

5.4 Detection of weld defects

The welded defect images generated by the improved WGAN-GP network are used as the test dataset. After the prediction of the YOLO-V4 target detection model, the detection and recognition effects of defects are shown in Fig. 7.

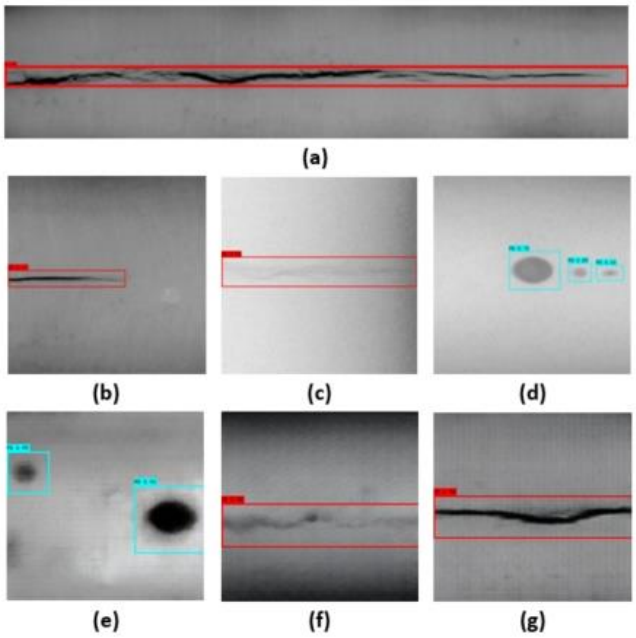

Fig. 7 The detection and recognition effects of defects. (a-d) The original welded defects; (e-g) WGAN-GP network.

Fig. 7 (a-d) shows the detection effects of the original welded defect samples. Fig. 7 (e-g) shows the detection effects of the samples generated by the improved WGAN-GP model. From the detection results, it is not difficult to see that the method proposed in this paper combining the WGAN-GP network and YOLO-V4 model could detect the defect of cracks and pores in various x-ray images. Meanwhile, this method avoids the problem of manually designing features in traditional machine learning algorithms. In the process of detection, prior knowledge of any particular specialty is not necessary.

5.5 Performance verification

In order to further verify the algorithm proposed in this paper, the Faster RCNN [17] is used as a controlled experiment to evaluate the advantages of our defect detection method. At present, the RCNN model and the YOLO model are the two most representative networks in the object detection field. Table 4 shows the performance comparison of the Faster RCNN model and the YOLO-V4 model.

Table 4

The performance comparison of various model

Parameters	Faster RCNN	The proposed model
F1 score (CR)	0.81	0.87
F1 score (PO)	0.79	0.85
mAP	83.50%	91.64%

It could be seen from Table 3 that the mAP of the Faster RCNN network and the YOLO-V4 network are 83.5% and 91.64%, So it is evident that the proposed method is more superior to the Faster RCNN network and is more in line with the needs of actual application scenarios.

6 Conclusion and future work

Face with weld defect detection on x-ray images, this paper proposes an automatic defect detection method using deep learning on a small weld X-ray image dataset. This method proposes two DCNN network models, which are used for data enhancement and defect detection, respectively. The main conclusions of this paper are as follows:

(1) In order to solve the problem of insufficient images of weld defects, the improved WGAN-GP is used to augment the dataset of real images, which meets the needs of the object detection model.

(2) To detect and locate the welded defects, the YOLO-V4 model is proposed that does not require handcrafted feature design and it achieves mAP result as 91.64%.

In the future, we will conduct research on more defect types and further improve the quality of images generated by the WGAN-GP model, strive to meet the needs of practical applications.

Acknowledgement

The work is supported by the National Natural Science Foundation of China (Grant No. 62073239).

R E F E R E N C E S

[1] R. Abdelkader, N. Ramou, M. Khorchef, et al, “Segmentation of x-ray image for welding defects detection using an improved Chan-Vese model”, in Materials Today: Proceedings, vol. 42, no. 5, Feb. 2021, pp. 2963-2967.

[2] X. Le, J. Mei, H. Zhang, et al, “A learning-based approach for surface defect detection using small image datasets”, in Neurocomputing, vol. 408, no. 30, Sept. 2020, pp. 112-120.

[3] D. Radi, M. Eldin A Abo-Elsoud, F. Khalifa, “Segmenting welding flaws of non-horizontal shape”, in Alexandria Engineering Journal, vol. 60, no. 4, Aug. 2021, pp. 4057-4065.

[4] Z. Xiao, K. Song, M. M. Gupta, “Development of a CNN edge detection model of noised X-ray images for enhanced performance of non-destructive testing”, in Measurement, vol. 174, Jan. 2021, pp. 109012-.
[5] W. M. Guo, H. F. Qu, L. H. Liang, “WDXI: The Dataset of X-Ray Image for Weld Defects”, in International Conference on Natural Computation, Fuzzy Systems and Knowledge Discovery (ICNC-FSKD), Huangshan, China, 2018.
[6] A. Krizhevsky, I. Sutskever, G. E. Hinton, “ImageNet classification with deep convolutional neural networks”, in Communications of the ACM, vol. 60, no. 6, Jun. 2017, pp. 84-90.
[7] K. Simonyan, A. Zisserman, “Very Deep Convolutional Networks for Large-Scale Image Recognition”, in International Conference on Learning Representations, San Diego, America, 2015.
[8] C. Szegedy, W. Liu, Y. Q. Jia, et al, “Going deeper with convolutions”, in 2015 IEEE Conference on Computer Vision and Pattern Recognition (CVPR), Boston, America, 2015.
[9] W. Z. Du, H. Y. Shen, J. Z. Fu, et al, “Approaches for improvement of the X-ray image defect detection of automobile casting aluminum parts based on deep learning”, in NDT and E International, vol. 107, Oct.2019, pp.102144.1-102144.12.
[10] L. Yang, Y. H. Liu, J. Z. Peng, “An Automatic Detection and Identification Method of Welded Joints Based on Deep Neural Network”, in IEEE ACCESS, vol. 7, Nov. 2019, pp.164952-164961.
[11] I. J. Goodfellow, J. Pouget-Abadie, M. Mirza, et al, “Generative Adversarial Networks”, in Advances in Neural Information Processing Systems, vol. 3, Jun.2014, pp.2672-2680.
[12] I. Gulrajani, F. Ahmed, M. Arjovsky, et al, “Improved Training of Wasserstein GANs”, in arXiv e-prints, 2017: 1704.00028.
[13] D. Mery, V. Riffo, U. Zscherpel, et al, “GDXray: The Database of X-ray Images for Nondestructive Testing”, in Journal of Nondestructive Evaluation, vol. 34, no. 4, Dec.2015, pp. 1-12.
[14] A. Bochkovskiy, C. Wang, H. M. Liao, “YOLOv4: Optimal Speed and Accuracy of Object”, in arXiv e-prints, 2020: 2004.10934.
[15] J. Redmon, A. Farhadi, “YOLOv3: An Incremental Improvement”, in arXiv e-prints, 2018: 1804.02767.
[16] T. Lin, P. Dollár, R. Girshick, et al, “Feature Pyramid Networks for Object Detection”, in arXiv e-prints, 2016: 1612.03144.
[17] S. Q. Ren, K. M. He, G. Ross, et al, “Faster R-CNN: Towards Real-Time Object Detection with Region Proposal Networks”, in IEEE Transactions on Pattern Analysis and Machine Intelligence, vol. 39, no. 6, Jun.2017, pp.1137-1149.